



Pictorial essay *Neuroradiology/Head and Neck Imaging*

Intracranial cerebrovascular lesions on T2-weighted magnetic resonance imaging

Navpreet Kaur R. Khurana¹, Eytan Raz², Atif Wasim Haneef Mohamed³, Houman Sotoudeh³, Amulya Reddy⁴, Jesse Jones⁵, Manoj Tanwar³

¹Department of Internal Medicine, Saint Vincent Hospital, Worcester, ²Department of Radiology, New York University Grossman School of Medicine, New York, ³Department of Neuroradiology, The University of Alabama at Birmingham, Birmingham, Alabama, ⁴Department of Internal Medicine, MedStar Health-Georgetown/Washington Hospital Center, Washington, DC, ⁵Department of Neurosurgery, The University of Alabama at Birmingham, Birmingham, Alabama, United States.



***Corresponding author:**

Navpreet Kaur R. Khurana,
Department of Internal
Medicine, Saint Vincent
Hospital, Worcester,
United States.

rhythmkhurana@gmail.com

Received: 20 February 2024

Accepted: 20 April 2024

Published: 19 June 2024

DOI

10.25259/JCIS_16_2024

Quick Response Code:



ABSTRACT

Magnetic resonance imaging (MRI) of the brain has been implemented to evaluate multiple intracranial pathologies. Non-contrast T2-weighted images are a routinely acquired sequence in almost all neuroimaging protocols. It is not uncommon to encounter various cerebrovascular lesions incidentally on brain imaging. Neuroradiologists should evaluate the routine T2-weighted images for incidental cerebrovascular lesions, irrespective of the primary indication of the study. Vascular structures typically demonstrate a low signal flow-void on the T2-weighted images. In our experience, large cerebrovascular abnormalities are easily visible to a typical neuroradiologist. In this article, we present the spectrum of the characteristic imaging appearance of various intracranial cerebrovascular lesions on routine non-contrast T2-weighted MRI. These include aneurysm, arteriovenous malformation, arterial occlusion, capillary telangiectasia, cavernous malformation, dural arteriovenous fistula, moyamoya, proliferative angiopathy, and vein of Galen malformation.

Keywords: Cerebrovascular, Incidental findings, Magnetic resonance imaging, Non-invasive imaging, Opportunistic screening

INTRODUCTION

Cerebrovascular lesions are a major cause of mortality and morbidity and affect a large number of patients seeking neurological care. For instance, in 2020, every 40 s someone in the United States had a stroke, and every 3.5 min someone died of a stroke; resulting in more than 795,000 annual cases of stroke in the United States. Neuroradiologists commonly encounter cerebrovascular abnormalities on magnetic resonance imaging (MRI), including the incidental discovery of various intracranial vascular lesions on imaging performed for myriad indications, with conventional unenhanced T2-weighted images acquired as a routine sequence.

In spin-echo imaging, the protons in flowing fluid move out of the plane of radiofrequency pulses between the initial excitation pulse and the refocusing pulse. This movement, known as the time-of-flight effect, causes the protons to miss the refocusing pulse and dephase, resulting in no signal contribution to that specific voxel. The extent of signal loss depends on the velocity of the protons moving out of the imaging plane, slice thickness, and time to echo (TE). In addition, signal loss can occur due to spin-phase effects caused by motion within the same imaging plane. The velocity of blood varies at different points within a vessel, leading to protons acquiring

This is an open-access article distributed under the terms of the Creative Commons Attribution-Non Commercial-Share Alike 4.0 License, which allows others to remix, transform, and build upon the work non-commercially, as long as the author is credited and the new creations are licensed under the identical terms.

©2024 Published by Scientific Scholar on behalf of Journal of Clinical Imaging Science

distinct phases as they traverse the applied gradient used for spatial encoding. The phase shift is determined by the proton's velocity, gradient strength, and TE. These differences cause signal loss within a voxel due to spin dephasing at a microscopic level.

Vascular structures typically demonstrate a low signal flow-void on T2-weighted images. T2 and proton-density sequences with a long TE demonstrate the most prominent flow voids. In our experience, large cerebrovascular abnormalities are easily evident. Thus, neuroradiologists should evaluate all T2-weighted images for incidental cerebrovascular lesions, irrespective of the primary indication of the study, and may recommend further evaluation with follow-up computed tomography, magnetic resonance (MR), or conventional angiogram as appropriate. In this article, we present the characteristic imaging appearance of various cerebrovascular lesions of the brain on routine non-contrast T2-weighted MRI [Table 1].

DISCUSSION

Aneurysm

Intracranial aneurysm rupture accounts for 0.4–0.6% of total deaths, with aneurysmal subarachnoid hemorrhage affecting

approximately 30,000 people every year in North America. Saccular aneurysms are the most common with about 85% located in the anterior circulation of the Circle of Willis, affecting the anterior communicating artery (35%), the internal carotid artery (30%), and the middle cerebral artery (MCA) (22%).^[1] Features on T2-weighted images typically include T2 hypointense outpouching along with an internal laminated thrombus with hyperintense rim evident in some cases [Figure 1].^[2]

Arteriovenous malformation (AVM)

Diagnostic criteria for AVM include the presence of a nidus embedded within the brain parenchyma, identified on either cross-sectional imaging or conventional angiography, and early venous drainage, which is best seen in dynamic studies. On T2-weighted MR, large lesions will be evident with a nidus and adjacent dilated vessels as well as numerous serpiginous flow voids generated due to fast flow [Figure 2]. Some small AVMs may only be seen on T2-weighted sequences as flow voids.^[3]

Table 1: Cerebrovascular lesion characteristics on conventional T2-weighted imaging.

Cerebrovascular lesion	T2-weighted imaging characteristics
Aneurysm	Hypointense outpouching with presence of internal laminated thrombus in some patients
Arteriovenous malformation	Heterogeneous signal nidus with adjacent hypointense draining vessels
Total arterial occlusion	Asymmetric loss of, or abnormal flow void, with loss of normal hypointensity
Capillary telangiectasia	Most commonly subtle hyperintense lesion
Cavernous malformation	“Popcorn” or “berry” appearance with a rim of signal loss
Dural arteriovenous fistula	Dilated arteries and brain without intervening nidus
Moyamoya disease	Stenosis of the carotid terminus and proximal middle cerebral artery, with distal arterial reconstitution
Proliferative angiopathy	Tangle of vessels and adjacent dilated supplying arteries and draining vein, without intervening abnormal brain tissue
Vein of galen malformation	Flow voids are seen with a dilated median prosencephalic vein
Vascular tumors	Hyperintense hemorrhagic foci interspersed with flow voids
Arterial atherosclerosis	Narrowed lumen appearing as flow voids within hyperintense plaque components

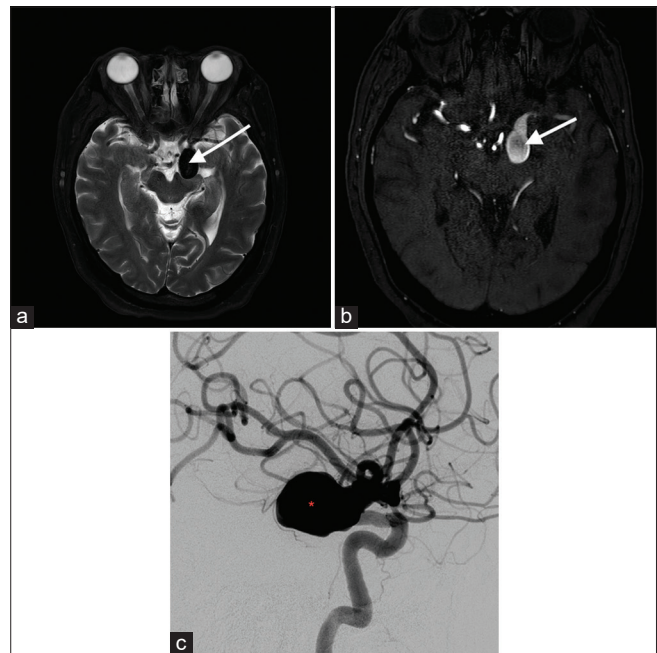


Figure 1: A 68-year-old female with left carotid terminus aneurysm. (a) Axial T2-weighted image shows a lobulated T2 hypointense lesion (white arrow) projecting posteriorly from the left carotid terminus. (b) Time-of-flight magnetic resonance angiogram confirms the lesion originating from the left carotid terminus, and hence an aneurysm (white arrow). (c) Conventional catheter angiogram with the left carotid injection demonstrates opacification of the posteriorly projecting berry aneurysm (red asterisk) originating from the distal carotid artery.

Arterial occlusion

Total arterial occlusion refers to a flow signal termination on all sequences at any point along the intracranial or extracranial artery. A focal gap in flow is evident with near-occlusions. Features on T2-weighted images include asymmetric loss of flow void, with loss of normal hypointensity [Figure 3].^[4]

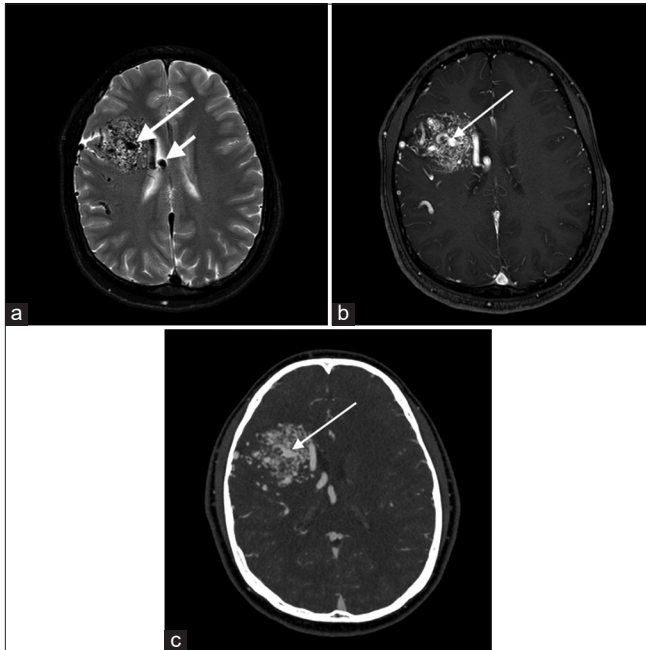


Figure 2: A 20-year-old male with the right frontal arteriovenous malformation (AVM). (a) Axial T2-weighted image shows a T2 heterogeneous signal nidus (long white arrow) in the right frontal lobe with dilated adjacent T2 hypointense vessels (short white arrow). (b) Axial T1+C image demonstrates a heterogeneously enhancing lesion (long white arrow) with adjacent dilated vessels. (c) Computed tomography angiogram confirms a right frontal AVM nidus (long white arrow) with a centrally draining vein medially.

These patients can be asymptomatic or present with transient ischemic attack or stroke symptoms.

Capillary telangiectasia

Capillary telangiectasia is low-flow lesions that are most commonly found in the brainstem, the majority being asymptomatic. They are usually discovered incidentally on imaging. On T2-weighted images, they are nearly always slightly hyperintense [Figure 4]. T2-weighted images may show low-signal intensity which is thought to be due to deoxyhemoglobin from sluggish flow, and not hemorrhage.^[5]

Cavernous malformations

Slow-flow venous malformations, majority are asymptomatic and are found incidentally on imaging. Tend to be supratentorial but can be found anywhere including the brainstem. They are usually solitary, although up to one-third of patients with sporadic lesions have more than one lesion. T2-weighted images demonstrate a characteristic “popcorn” or “berry” appearance with a peripheral rim of signal loss due to the presence of hemosiderin [Figure 5].^[6]

Dural Arteriovenous (AV) fistulas

These are pathologic connections between dural arteries and dural veins, meningeal veins, or cortical veins, distinguished from parenchymal or pial AVMs by the presence of a dural arterial supply and the absence of a parenchymal nidus.^[7] On T2-weighted MR, numerous dural or leptomeningeal flow voids, venous ectasia, or regionally increased leptomeningeal flow voids are considered key findings, with white matter hyperintensity and intracranial hemorrhage possibly representing sequelae of fistulae [Figure 6]. In cavernous sinus dural arteriovenous fistula, large flow voids within the sinus are best visualized on T2-weighted sequences.

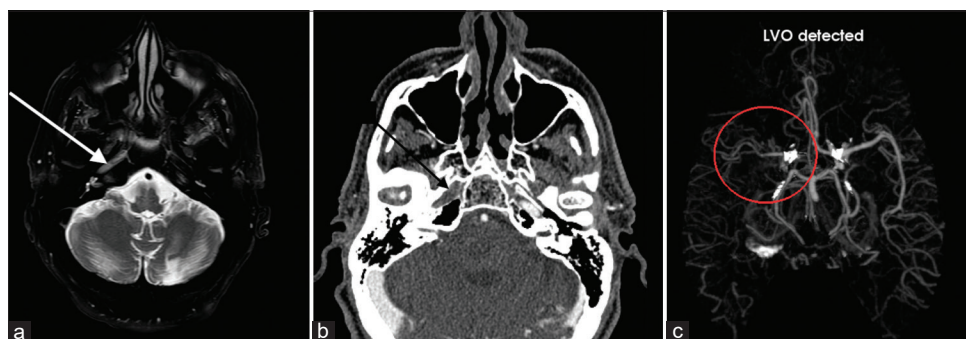


Figure 3: A 64-year-old male with the right internal carotid artery (ICA) occlusion. (a) Axial T2-weighted image shows absence of flow void (white arrow) in the petrous segment of the right ICA which is worrisome for arterial occlusion. (b) Computed tomography angiogram confirms lack of contrast related enhancement in the right petrous ICA (black arrow) consistent with occlusion. (c) Furthermore, AI detection platform detects this large vessel occlusion as well (red circle). LVO: Large vessel occlusion, AI: Artificial intelligence.

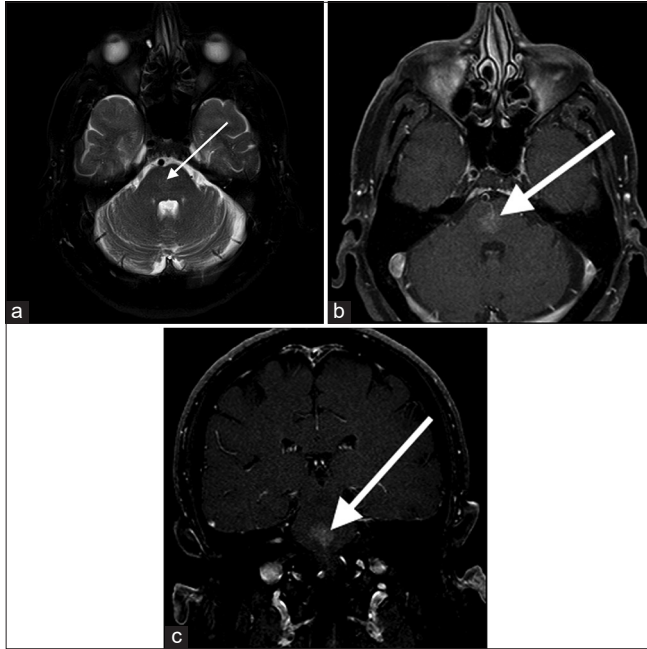


Figure 4: A 65-year-old male with pontine capillary telangiectasia. (a) Axial T2-weighted image shows a faint T2 hyperintense lesion in the pons (white arrow), and suggestive of an underlying vascular lesion. (b and c) Axial and coronal T1+C images demonstrate a faint enhancing lesion (white arrows) in the pons consistent with capillary telangiectasia.

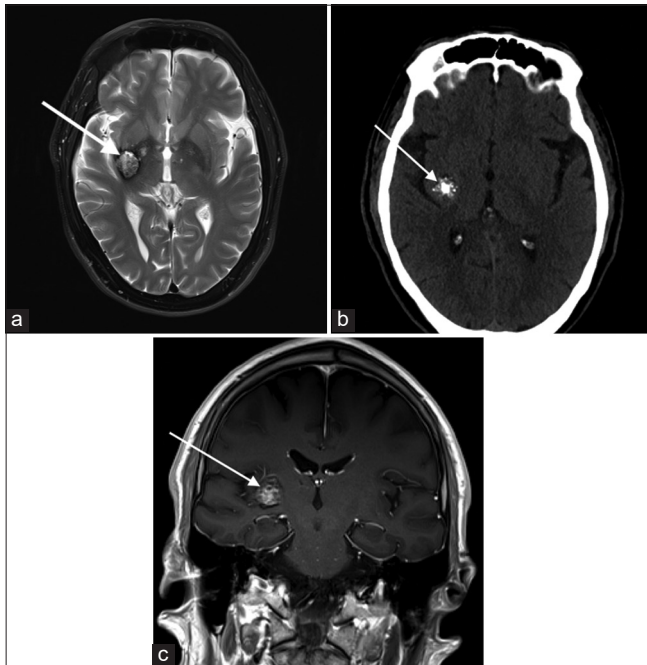


Figure 5: A 67-year-old male with the right basal ganglia cavernous malformation. (a) Axial T2-weighted image shows a popcorn shaped lesion (white arrow) in the right posterior putamen and globus pallidum with a peripheral hypointense rim. (b) Non-contrast head computed tomography demonstrates internal calcifications (white arrow). (c) Lesion shows internal heterogeneous enhancement (white arrow) on the coronal T1+C image. Combination of these imaging findings is consistent with a cavernous malformation.

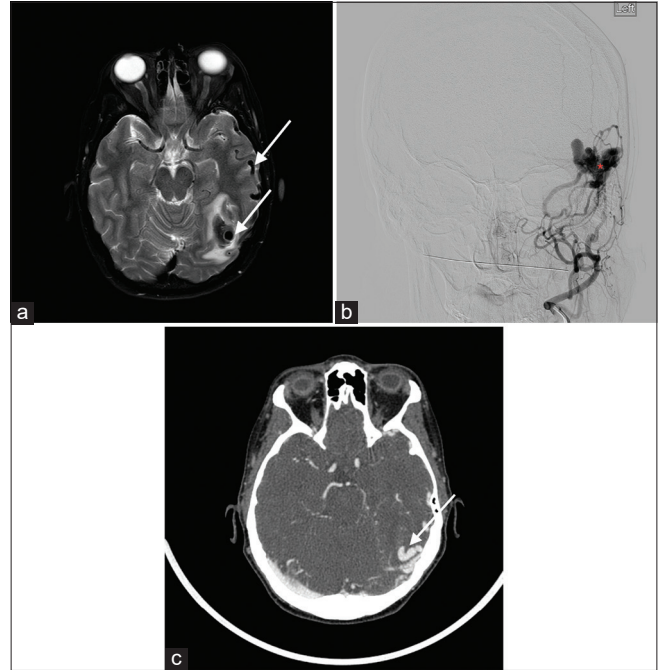


Figure 6: A 52-year-old female with the left temporal dural arteriovenous fistula (dAVF). (a) Axial T2-weighted image shows a T2 hypointense lesion (long white arrow) in the posterior left temporal lobe with adjacent dilated cortical veins (short white arrow) and surrounding edema, worrisome for an underlying vascular lesion. (b) Conventional catheter angiogram confirms Borden 3 left tentorial dAVF (red asterisk) with multiple arterial pedicles arising from the left external carotid artery (left Medial Meningeal Artery (MMA), left occipital/posterior auricular arteries). (c) Axial computed tomography angiogram image again demonstrates these findings (white arrow). MMA: Medial meningeal artery.

Moyamoya disease

Japanese for “puff of smoke,” Moyamoya disease refers to the unilateral or bilateral stenosis or occlusion of carotid termini and proximal M1 segment MCAs, with further associated prominent arterial collateral formation. Leptomeningeal collaterals resulting in contrast enhancement and high signal on fluid attenuated inversion recovery (FLAIR) is known as the “Ivy sign.” Features on T2-weighted images include stenosis of the carotid terminus and proximal MCA [Figure 7].^[8]

Proliferative angiopathy

Cerebral proliferative angiopathy is a rare, relatively newly described cerebrovascular malformation that comprises the feeding arteries, nidus, and draining veins. One important feature distinguishing it from AVMs is the presence of normal brain parenchyma in-between the abnormal vascular channels. In contrast to AVMs, the natural history of the disease suggests a lower risk

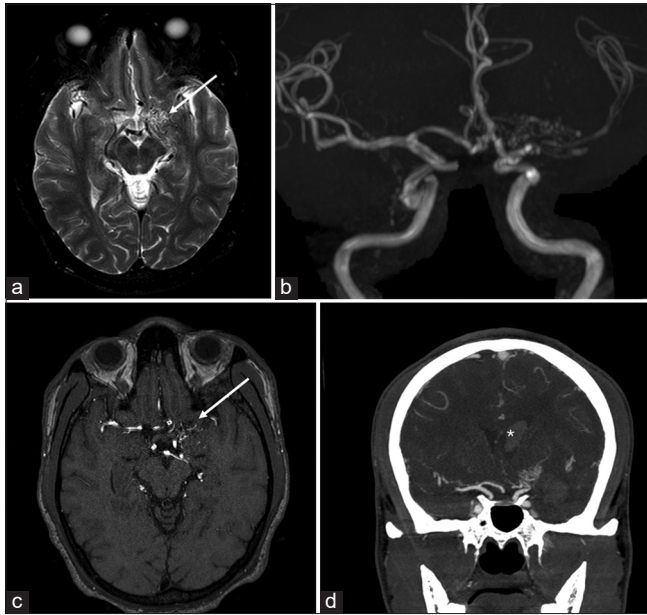


Figure 7: A 29-year-old female with Moyamoya. (a) Axial T2-weighted image show a cluster of vessels in the expected location of the proximal M1 segment of the left middle cerebral artery (MCA), (white arrow), and poor visualization of the carotid terminus, raising concern for underlying Moyomoya. (b) Time-of-flight magnetic resonance angiogram (MRA) confirms multiple small collateral vessels in this region. (c) 3D-rendered MRA image further confirms these findings (white arrow), with also right carotid and MCAs shown for comparison. (d) These findings are also evident on coronal maximal intensity projection computed tomography angiogram image, which also demonstrate intraventricular hemorrhage (white asterisk), which is one of the complications of Moyamoya disease. R stands for right, L stands for left.

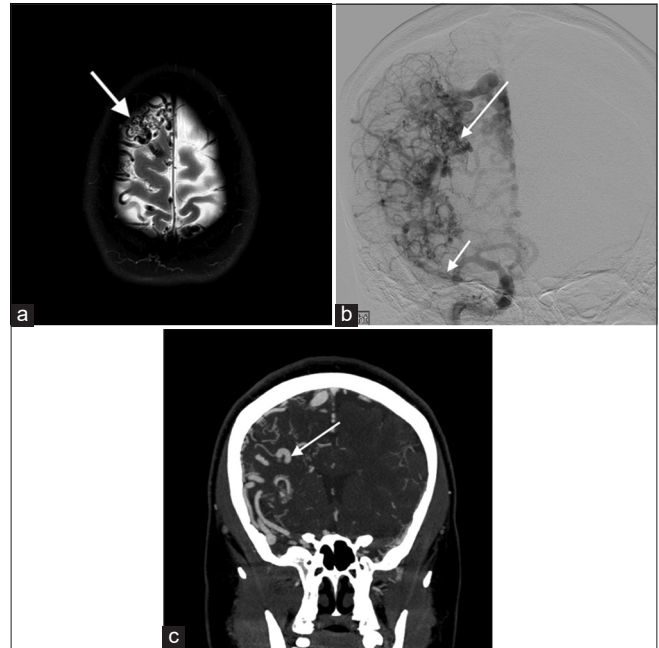


Figure 8: A 35-year-old female with proliferative angiopathy. (a) Axial T2-weighted image shows multiple dilated T2 hypointense vessels in and along the right frontal lobe, a nidus (white arrow) and normal adjacent brain parenchyma. Findings are suggestive of a proliferative angiopathy. (b) Conventional catheter angiogram shows a larger (>3 cm) nidus (long arrow) and multiple prominent arterial feeders (short white arrow). (c) Computed tomography angiogram demonstrates abnormal vessels originating from right anterior and middle cerebral arteries (white arrow). Findings are consistent with proliferative angiopathy.

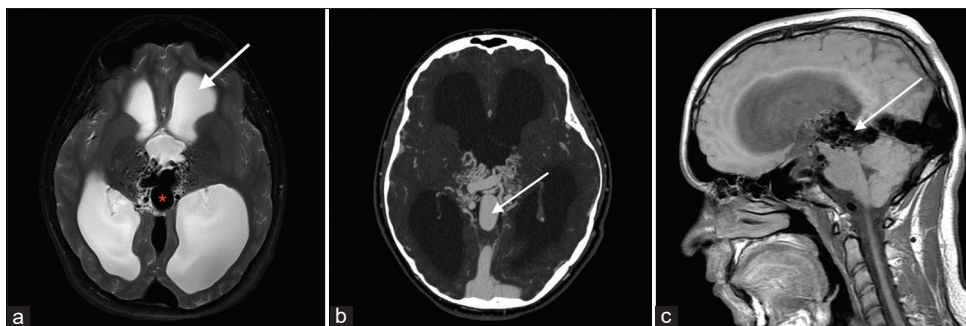


Figure 9: A 17-year-old male with vein of Galen malformation. (a) Axial T2-weighted image shows a tangled mass of abnormal connection of the arteries and the median prosencephalic vein of Markowski (white arrow). There is also associated moderate hydrocephalus (red asterisk). (b) Computed tomography angiogram demonstrates opacification of the abnormal vessels and medial prosencephalic vein (white arrow). (c) Sagittal T1-weighted image further confirms the findings (white arrow).

of hemorrhage, which makes differentiation clinically important. T2-weighted images show a tangle of vessels with adjacent dilated supplying arteries and draining veins [Figure 8].

Vein of Galen malformation

Vein of Galen malformation is a congenital AV fistula involving the median prosencephalic vein of Markowski.

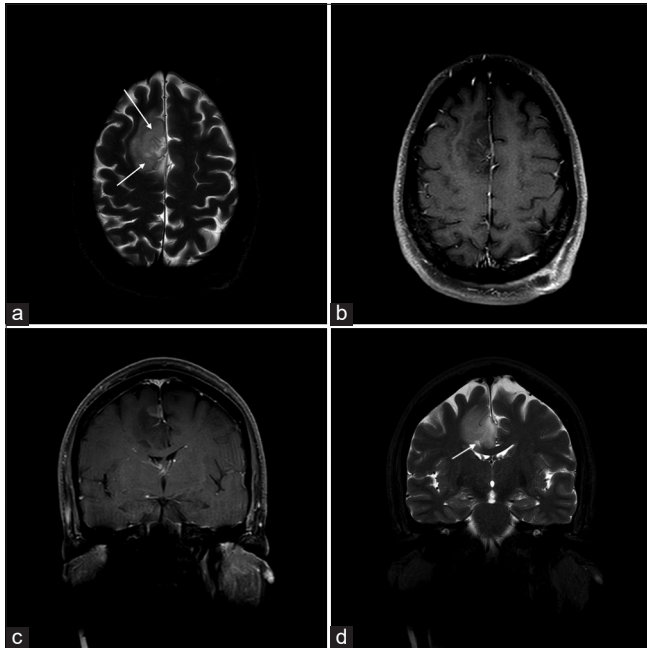


Figure 10: A 45-year-old male with anaplastic astrocytoma grade III, with IDH ½ mutation. (a) Axial and (b) coronal T2-weighted images show a T2 hyperintense mass centered on the left superior frontal gyrus. Internal vessels are evident as curvilinear dark flow voids (white arrows). On the (c) axial and (d) coronal T1+C images, mass is predominantly non-enhancing, with a small enhancing nodular component (asterisk). Previously seen vascular flow voids correspond to linear foci of enhancement (white arrows). IDH: Isocitrate dehydrogenase.

Lasjaunias classification further describes choroidal and mural types. Signal abnormalities including T2 prolongation and flow voids in periventricular regions are seen on T2-weighted imaging with a dilated median prosencephalic vein, the name of vein of Galen is a misnomer [Figure 9].^[9]

Vascular tumors

Astrocytomas are hyperintense on T2-weighted images with ill-defined borders, and a T2-FLAIR mismatch sign is indicative of isocitrate dehydrogenase (IDH)-mutant subtype.^[10] IDH mutations, crucial prognostic markers, confer better outcomes, distinguishing them from aggressive glioblastomas [Figure 10]. Oligodendrogliomas with intact 1p/19q show homogeneous T1/T2 signals with sharp borders, differing from “true” oligodendrogliomas with codeletion. Lesions with well-circumscribed T1 hypointensity, high T2 signal, and T2/FLAIR mismatch predict absence of 1p19q codeletion [Figure 11].^[11] Calcification and hemorrhage appear as signal loss on T2* sequences; contrast enhancement is common but unreliable for grading. Diffusion weighted imaging (DWI) and MR perfusion aid in distinguishing oligodendrogliomas from astrocytomas based on vascularity and cellularity. T2-weighted imaging can help in the assessment of presence of large internal vessels while planning surgical resection.

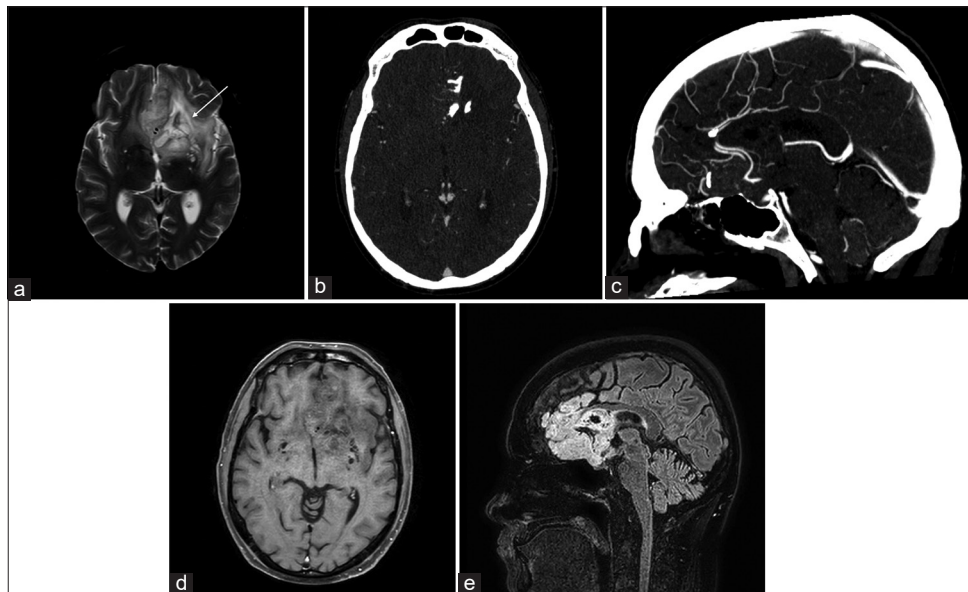


Figure 11: A 39-year-old male with anaplastic oligodendroglioma, with 1p/19q codeleted, IDH mutation. (a) Axial T2-weighted image shows a left frontal mass which encases the traversing bilateral anterior cerebral arteries (white arrow). (b) Axial and (c) sagittal computed tomography angiogram demonstrates characteristics internal calcifications in the mass and confirms the presence of ACAs medially. The ACA flow voids are also evident on the (d) axial T1+C and (e) sagittal FLAIR images. IDH: isocitrate dehydrogenase, ACA: Anterior cerebral artery, FLAIR: Fluid-attenuated inversion recovery.

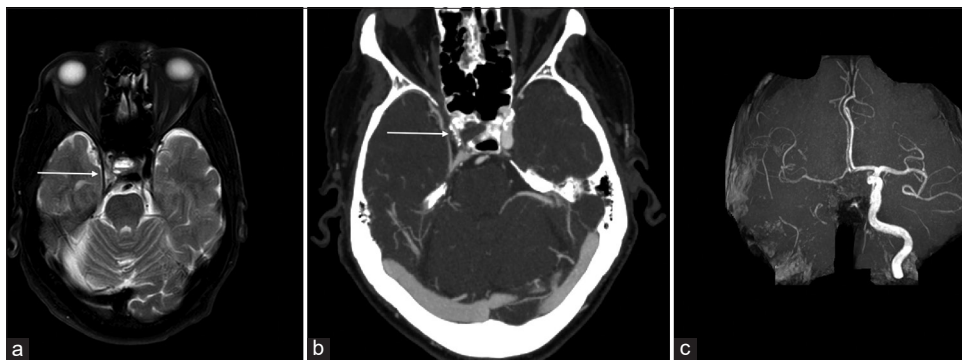


Figure 12: A 75-year-old male with severe atherosclerotic plaque in the right internal carotid artery (ICA). (a) Axial T2-weighted image shows an asymmetrically luminal diameter of the supraclinoid segment of the right ICA (white arrow). There is also associated moderate hydrocephalus. (b) Computed tomography angiogram demonstrates severe short-segment stenosis in the cavernous and supraclinoid segments of the right ICA, with associated calcified plaque (white arrow). (c) Maximal intensity projection time-of-flight magnetic resonance angiogram image further confirms the severely diseased right ICA.

Arterial atherosclerosis

Narrowing of the arterial lumen can be evident as flow voids on T2-weighted sequences. The plaque components-fibrous cap, intraplaque hemorrhage, and juxtaluminal thrombus-demonstrate a hyperintense T2 signal that can be visualized adjacent to the flow void on T2-weighted sequences [Figure 12]. Calcification and hemosiderin within the plaque appear hypointense on T2. Yu *et al.*^[12] demonstrated that MCA plaque hyperintensity on T2-weighted images (>50% stenosis) was associated with symptomatic MCA plaque, and a normalized plaque signal of 1.3–1.4 provided the highest diagnostic value for symptomatic plaque.

CONCLUSION

Incidental discovery of intracranial cerebrovascular lesions can lead to early diagnosis and further optimal management of complex vascular lesions. Routinely acquired T2-weighted imaging can be utilized as an essential sequence to look for vascular lesions, commonly appearing as flow voids with characteristic shapes and imaging appearances. Knowledge of pathophysiology, clinical presentation, and characteristic imaging findings of cerebrovascular lesions is imperative to improve their detection rate, which can prevent future adverse events in selected patients.

Ethical approval

The Institutional Review Board approval is not required.

Declaration of patient consent

Patients' consent not required as patients' identity is not disclosed or compromised.

Financial support and sponsorship

Nil.

Conflicts of interest

There are no conflicts of interest.

Use of artificial intelligence (AI)-assisted technology for manuscript preparation

The authors confirm that there was no use of artificial intelligence (AI)-assisted technology for assisting in the writing or editing of the manuscript and no images were manipulated using AI.

REFERENCES

1. Keedy A. An overview of intracranial aneurysms. *McGill J Med* 2006;9:141-6.
2. Chung CY, Peterson RB, Howard BM, Zygmunt ME. Imaging intracranial aneurysms in the endovascular era: Surveillance and posttreatment follow-up. *Radiographics* 2022;42:789-805.
3. Geibprasert S, Pongpech S, Jiarakongmun P, Shroff MM, Armstrong DC, Krings T. Radiologic assessment of brain arteriovenous malformations: What clinicians need to know. *Radiographics* 2010;30:483-501.
4. Sato K, Hijikata Y, Omura N, Miki T, Kakita H, Yoshida T, *et al.* Usefulness of three-dimensional fast imaging employing steady-state acquisition MRI of large vessel occlusion for detecting occluded middle cerebral artery and internal carotid artery before acute mechanical thrombectomy. *J Cerebrovasc Endovasc Neurosurg* 2021;23:201-9.
5. Lee RR, Becher MW, Benson ML, Rigamonti D. Brain capillary telangiectasia: MR imaging appearance and clinicohistopathologic findings. *Radiology* 1997;205:797-805.
6. Wang KY, Idowu OR, Lin DD. Radiology and imaging for

- cavernous malformations. *Handb Clin Neurol* 2017;143:249-66.
7. Kwon BJ, Han MH, Kang HS, Chang KH. MR imaging findings of intracranial Dural arteriovenous fistulas: Relations with venous drainage patterns. *AJNR* 2005;26:2500-7.
 8. Li J, Jin M, Sun X, Li J, Liu Y, Xi Y, *et al.* Imaging of moyamoya disease and moyamoya syndrome: Current status. *J Comput Assist Tomogr* 2019;43:257-63.
 9. Kortman H, Navaei E, Raybaud CA, Bhatia KD, Shroff M, terBrugge K, *et al.* Deep venous communication in vein of Galen malformations: Incidence, imaging, and implications for treatment. *J Neurointerv Surg* 2021;13:290-3.
 10. Park SI, Suh CH, Guenette JP, Huang RY, Kim HS. The T2-FLAIR mismatch sign as a predictor of IDH-mutant, 1p/19q-noncodeleted lower-grade gliomas: A systematic review and diagnostic meta-analysis. *Eur Radiol* 2021;31:5289-99.
 11. Johnson DR, Diehn FE, Giannini C, Jenkins RB, Jenkins SM, Parney IF, *et al.* Genetically defined oligodendroglioma is characterized by indistinct tumor borders at MRI. *AJNR Am J Neuroradiol* 2017;38:678-84.
 12. Yu YN, Liu MW, Villablanca JP, Li ML, Xu YY, Gao S, *s.* Middle cerebral artery plaque hyperintensity on T2-weighted vessel wall imaging is associated with ischemic stroke. *AJNR Am J Neuroradiol* 2019;40:1886-92.

How to cite this article: Khurana NR, Raz E, Mohamed A, Sotoudeh H, Reddy A, Jones J, *et al.* Intracranial cerebrovascular lesions on T2-weighted magnetic resonance imaging. *J Clin Imaging Sci.* 2024;14:19. doi: 10.25259/JCIS_16_2024